

Habitability around F-type Stars

S. Sato¹, M. Cuntz¹, C. M. Guerra Olvera², D. Jack², K.-P. Schröder²

¹*Department of Physics, University of Texas at Arlington, Arlington, TX 76019, USA*

²*Department of Astronomy, University of Guanajuato, 36000 Guanajuato, GTO, Mexico*

satoko.sato@mavs.uta.edu; cuntz@uta.edu; cguerra@astro.ugto.mx;
dennis@astro.ugto.mx; kps@astro.ugto.mx

ABSTRACT

We explore the general astrobiological significance of F-type main-sequence stars with masses between 1.2 and 1.5 M_{\odot} . Special consideration is given to stellar evolutionary aspects due to nuclear main-sequence evolution. DNA is taken as a proxy for carbon-based macromolecules following the paradigm that extraterrestrial biology may be most likely based on hydrocarbons. Consequently, the DNA action spectrum is utilized to represent the impact of the stellar UV radiation. Planetary atmospheric attenuation is taken into account based on parameterized attenuation functions. We found that the damage inflicted on DNA for planets at Earth-equivalent positions is between a factor of 2.5 and 7.1 higher than for solar-like stars, and there are intricate relations for the time-dependence of damage during stellar main-sequence evolution. If attenuation is considered, smaller factors of damage are obtained in alignment to the attenuation parameters. This work is motivated by earlier studies indicating that the UV environment of solar-type stars is one of the most decisive factors in determining the suitability of exosolar planets and exomoons for biological evolution and sustainability.

Subject headings: extra-solar planets, extraterrestrial life, F-type stars, habitable zone, planetary climate and stellar evolution.

1. Introduction

Omitting O and B-type stars in consideration of their short lifespans and strong ionizing winds (e.g., Maeder & Meynet 1988; Kudritzki & Puls 2000), as well as the transitory case of A-type stars, F-type main-sequence stars represent the hot limit of stars with a significant potential for providing circumstellar habitable environments (e.g., Kasting *et al.* 1993;

Underwood *et al.* 2003). Generally, the investigation of habitability around different types of stars, particularly main-sequence stars, is considered a theme of pivotal interest to the thriving field of astrobiology; see, e.g., Jones (2008), Lammer *et al.* (2009), Kaltenegger *et al.* (2010), Horner & Jones (2010), and Lammer *et al.* (2013) for previous studies and reviews. For planetary host stars — like any other star — the stellar mass determines their lifetime (shorter with larger mass), luminosity and effective temperature (both higher with larger mass). Main-sequence stars moderately more massive than the Sun with masses between 1.1 and 1.6 M_{\odot} , i.e., F-type stars, are of particular interest as hosts to exosolar planets and exomoons in orbit about those planets. Compared to stars of later spectral types, F-type stars are characterized by relatively large habitable zones, although from a general astrobiological point of view, they exhibit the adverse statistical property of being less frequent (e.g., Kroupa 2002; Chabrier 2003). On the other hand, despite their reduced lifetimes compared to G-type stars, their lifetimes still exceed several billion years (e.g., Maeder & Meynet 1988), allowing the principle possibility of exobiology, potentially including advanced life forms.

While habitable zones and their evolution can, in general, be well characterized in terms of the total amount of stellar irradiation, the spectral energy distribution (including its portion of energetic radiation) may nevertheless be significant as well for the facilitation of habitability (e.g., Lammer *et al.* 2009). The emergent radiation of F-type stars consists of significantly larger amounts of UV compared to the Sun thus entailing potentially unfavorable effects on planetary climates and possible organisms (e.g., Cockell 1999). Previous studies showed that increased levels of UV, as well as the even more energetic EUV radiation, can trigger a variety of chemical planetary atmospheric processes, including exoplanetary atmospheric evaporation (e.g., Guinan & Ribas 2002; Lammer *et al.* 2003; Güdel 2007). Hence, the radiation output provided by F-stars places an additional constraint on circumstellar habitability, which needs to be considered as part of more comprehensive assessments; see, e.g., Buccino *et al.* (2006) for previous results. It is the aim of the present study to consider some of these processes in an approximate manner while also taking into account the evolutionary status of the F-type host stars.

In Sect. 2, we comment on the concept of habitability, which also includes a description of the climatological habitable zone. Additionally, we discuss the governing equations of the present study involving both the DNA action spectrum and planetary atmospheric attenuation. In Sect. 3, we describe the spectral energy distribution of the host stars based on sophisticated photospheric models and their spectral energy output computed by the PHOENIX code for the range of effective temperatures relevant to F-type stars. The specific effective temperature and total luminosity of each star for a given mass and age are derived from well-tested stellar evolution models, which also convey the time scales of the circumstellar conditions during stellar main-sequence evolution as well as the extents of the

climatological habitable zones. Results and discussion are given in Sect. 4, which focuses on habitability gauged by the damage inflicted upon DNA. Particular emphasis is placed on the relevance of the different types of UV (i.e., UV-A, UV-B, and UV-C; see Sect. 2.2 for definitions). Our summary and conclusions are given in Sect. 5.

2. Concepts of Habitability

2.1. Climatological Habitable Zone

A key aspect in the study of circumstellar habitability is the introduction of the climatological habitable zone, a concept, evaluated by Kasting *et al.* (1993). They utilized 1-D climate model to estimate the position and width of the habitable zone around solar-like stars as well as other types of main-sequence stars. The basic premise consists in assuming a Earth-like planet with a CO₂/H₂O/N₂ atmosphere and, furthermore, that habitability requires the presence of water on the planetary surface. In their work they distinguished between the *conservative* habitable zone (CHZ, with limits of 0.95 and 1.37 AU) and the *general* habitable zone (GHZ, with limits of 0.84 and 1.67 AU); subsequent work about the GHZ has also been given by Forget & Pierrehumbert (1997) and others¹.

The physical significance of the various kinds of HZs obtained by Kasting *et al.* (1993) are given as follows: The GHZ is defined as bordered by the runaway greenhouse effect (inner limit) and the maximum greenhouse effect (outer limit). Concerning the latter it is assumed that a cloud-free CO₂ atmosphere shall still be able to provide a surface temperature of 273 K. By contrast, the inner limit of the CHZ is defined by the onset of water loss. In this case, a wet stratosphere is assumed to exist where water is lost by photodissociation and subsequent hydrogen escape to space. Furthermore, the outer limit of the CHZ is defined by the first CO₂ condensation attained by the onset of formation of CO₂ clouds at a temperature of 273 K; see, e.g., Underwood *et al.* (2003) for additional details and applications.

Owing to the shape of the photospheric spectra and the total amount of the radiative energy fluxes, the limits of the habitable zones are known to depend both on the stellar effective temperatures T_{eff} and the luminosities L_* . The results for the CHZs and GHZs as well as the appropriate Earth-equivalent positions for main-sequence stars between spectral type F0 and G0 are given in Fig. 1. For F0 V stars, the CHZ extends between 2.27 and 2.92 AU

¹Alternate usages of the acronym CHZ include climatological habitable zone and continuous habitable zone. Also, an alternate usage of the acronym GHZ includes galactic habitable zone. However, those do not apply in this study.

and the GHZ extends between 1.99 and 3.67 AU. Furthermore, for F8 V stars, the CHZ extends between 1.29 and 1.80 AU and the GHZ extends between 1.14 and 2.21 AU. The corresponding stellar data are given in Table 1. They are those also adopted for the photospheric models computed with the PHOENIX code (see Sect. 3.1), which have subsequently been used for our astrobiological studies.

Another aspect of habitability concerns the limits of the climatological habitable zones for the various types of stars. They have been calculated based on the formalism by Selsis *et al.* (2007). It provides a suitable polynomial fit and, furthermore, implements the required correction for the solar effective temperature in consideration of that Kasting *et al.* (1993) used for an unusually low value of 5700 K instead of 5777 K as currently accepted.

2.2. Impact of UV: The DNA Action Spectrum

Next we comment on the relevance of the DNA action spectrum. The most fundamental radiometric technique to quantify radiative damage on biomolecules and microorganisms is spectroradiometry. Biological effectiveness spectra can be derived from spectral data by multiplication with an action spectrum $S_\lambda(\lambda)$ of a relevant photobiological reaction with the action spectrum typically given in relative units normalized to unity for, e.g., $\lambda = 300$ nm. The biological effectiveness for a distinct range of the electromagnetic spectrum such as UV radiation is determined by

$$E_{\text{eff}} = \int_{\lambda_1}^{\lambda_2} E_\lambda(\lambda) S_\lambda(\lambda) \alpha(\lambda) d\lambda \quad , \quad (1)$$

where $E_\lambda(\lambda)$ denotes the stellar irradiance ($\text{ergs cm}^{-2} \text{ s}^{-1} \text{ nm}^{-1}$), λ the wavelength (nm), and $\alpha(\lambda)$ the planetary atmospheric attenuation function; see Horneck (1995). Here λ_1 and λ_2 are the limits of integration which in our computations are set as 200 nm and 400 nm, respectively. Although a significant amount of stellar radiation exists beyond 400 nm, this portion of the spectrum is disregarded in the following owing to the minuscule values for the action spectrum $S_\lambda(\lambda)$ in this regime. Planetary atmospheric attenuation, sometimes also called extinction, results in a loss of intensity of the incident stellar radiation. In Eq. (1) $\alpha = 1$ indicates no loss and $\alpha = 0$ indicates a complete loss (see Sect. 2.3); note that $\alpha(\lambda)$ can be attained by various types of methods, which may also consider detailed atmospheric photochemical models.

Based on previous work, the UV region of the electromagnetic spectrum has been divided into three bands termed UV-A, UV-B, and UV-C. The subdivisions are somewhat

arbitrary and differ slightly depending on the discipline involved². Here we will use: UV-A, 400-320 nm; UV-B, 320-290 nm; and UV-C, 290-200 nm. Following Diffey (1991), the division between UV-B and UV-C is chosen as 290 nm since UV at shorter wavelengths is unlikely to be present in terrestrial sunlight, except at high altitudes (Henderson 1977). The choice of 320 nm as the division between UV-B and UV-A is suggested by the level of photobiological activity although subdivisions at 330 or 340 nm have previously also been advocated (Peak & Peak 1986).

In order to compute the irradiance toward targets in circumstellar environments, typically positioned in stellar habitable zones, a further equation is needed, which is

$$E_\lambda(\lambda) \propto F_\lambda(R_*/d)^2 \quad , \quad (2)$$

where F_λ is the stellar radiative flux, R_* is the stellar radius and d is the distance between the target and the star. In the framework of this work, we will focus on planets at different positions in stellar HZs. For stellar UV radiation we will consider photospheric radiation only (see Sect. 3) because the chromospheric UV radiation from F-type stars is of minor importance (Linsky 1980).

Action spectra for DNA, also to be viewed as weighting functions, have previously been utilized to quantify and assess damage due to UV radiation (Setlow 1974). Besides DNA, action spectra have also been derived for other biomolecules, for biostructures such as cellular components as well as for distinct species, especially extremophiles (e.g., Horneck 1995; Rettberg & Rothschild 2002, and references therein). Horneck (1995) provides information on the DNA action spectrum for the range from 285 nm (UV-C) to 400 nm (UV-A). She found that between 400 and 300 nm, the action spectrum increases by almost four orders of magnitude (see Fig. 2). The reason for this behavior is the wavelength-dependency of the absorption and ionization potential of UV radiation in this particular regime. A further significant increase in the DNA action spectrum occurs between 300 and 200 nm (see below). Fortunately, however, the Earth’s ozone layer is very sufficient to filter out this type of lethal radiation (e.g., Diffey 1991; Cockell 1998), which in our models is mathematically dealt with by considering an appropriate attenuation function $\alpha(\lambda)$ (see Eq. 1).

The behavior of the DNA action spectrum in the wavelengths regime between 200 and 290 nm has been given by Cockell (1999). He points out that a significant reason for the susceptibility to UV-induced damage are π -electron systems, notably because of their π to π^*

²Wavelengths above 380 nm are often considered already belonging to the optical regime, which is however inconsequential for this study in consideration of the very small values of the employed action spectrum between 360 and 400 nm.

energy transitions. It is found that this type of interaction also accounts for protein damage and damage to enzymes of photosynthesis, which indicates that these types of biochemical reactions are of general importance. The increase in the relative biological damage is about a factor of 35 relative to the damage at the reference wavelengths of 300 nm (see Fig. 2).

2.3. Planetary Atmospheric Attenuation

A relevant ingredient to our study is the consideration of planetary atmospheric attenuation $\alpha(\lambda)$, which typically results in a notable reduction of the received stellar radiation. Appropriate values for $\alpha(\lambda)$ can be obtained through the analysis of theoretical exoplanetary models (e.g., Meadows & Seager 2011; Kaltenegger et al. 2012), inspired by recent results from the *Kepler* mission, or the usage of historic Earth-based data (e.g., Cockell 2002). Within the scope of the present work that is mostly focused on the impact of photospheric radiation from stars of different spectral types, as well as on the role of active and inactive stellar chromospheres, we assume that $\alpha(\lambda)$ is given by a parameterized attenuation function ATT defined as

$$\text{ATT}(\lambda) = \frac{C}{2} \left[1 + \tanh(A(\lambda - B)) \right] ; \quad (3)$$

see Fig. 3 for a depiction of different examples (A, B, C). Here A denotes the start-of-slope parameter, B (in nm) the center parameter, and C the maximum (limited to unity) of the distribution.

For example, Cockell (2002) provided information about the ultraviolet irradiance reaching the surface of Archean Earth for various assumptions about Earth’s atmospheric composition; the latter allow us to constrain the wavelength-dependent attenuation coefficients for Earth 3.5 Gyr ago. Furthermore, there is a large array of recent studies about exosolar planetary atmospheres, including those for rocky planets. They encompass models regarding the detailed treatment of atmospheric photochemistry, including the build-up and destruction of ozone, as discussed by, e.g., Segura *et al.* (2003), Scalo *et al.* (2007) and Grenfell *et al.* (2007). These models provide information on different exoplanetary structures due to outside forcings, including variable stellar radiation, which in principle allow the derivation of detailed planetary atmospheric attenuation functions.

3. Stellar Evolution, Photospheric Models and Irradiance

3.1. Basic Properties

In accordance to previous studies of our group, as given by von Bloh *et al.* (2009) and Cuntz *et al.* (2012), which mostly focused on super-Earth planets, we rely again on selected stellar evolution models that have been computed with the well-tested Eggleton code; see, e.g., Schröder & Smith (2008) for a description of an adequate solar evolutionary model. The Eggleton code allows us to take into account the changing properties of the host star during its evolution on the main-sequence and, subsequently, as a red giant. We use an advanced version of the Eggleton code, including updated opacities and an improved equation of state as described by Pols *et al.* (1995, 1998). Besides other desirable characteristics, the adopted evolution code utilizes a self-adapting mesh and also permits treating “overshooting” — a concept of extra mixing, which has been thoroughly tested considering observational constraints. In particular, the two convection parameters, the “mixing length” and the “overshoot length”, have been calibrated by matching accurately the physical properties of various types of stars, including giants and supergiants of well-known masses, found in well-studied, eclipsing binary systems (Schröder *et al.* 1997).

For the abundance of heavy elements, which decisively affect the opacities, we use the near-solar value of $Z = 0.02$. This choice is an appropriate representation of present-day samples of stars in the thin galactic disk, noting that they exhibit a relatively narrow distribution ($Z = 0.01$ to 0.03) about this value. The adopted evolution code also considers a detailed and well-tested description of the stellar mass loss, which becomes important for the final stages of giant star evolution; see Schröder & Cuntz (2005) and Schröder & Cuntz (2007). Regarding our models of planetary host stars, the principal input parameters are the total luminosity and effective temperature, which are found to change with time. Obviously, the resulting total lifetime of the star is a quantity of high significance as well.

While the effective temperature and luminosity of the host star already allow a good representation of circumstellar habitability, as done through the stellar climatological habitable zone (see Sect. 2.1), the irradiation especially in the UV regime is of pivotal importance as well for arriving at a realistic evaluation of habitability. The main constraint arises from having sustainable conditions for biological organisms and biochemical processes, which provide the basis of life. Here, damaging ultraviolet radiation must be of particular concern. Its share regarding the total stellar luminosity critically depends on the stellar effective temperature and increases significantly from late (F9) to early (F0) F-type stars.

We employ the necessary and accurate account of stellar radiation, including its spectral energy distribution, by utilizing a number of photospheric models computed by the

PHOENIX code following Hauschildt (1992); see Fig. 4. The adopted range of models for the F-type stars are in response to effective temperatures of 7200 K for spectral type F0, 7000 K for F1, 6890 K for F2, 6700 K for F3, 6440 K for F5, 6200 K for F8, and 6050 K for G0. The PHOENIX code iterates the principal physics and structure of a stellar atmosphere until a final model is obtained, which is in radiative and hydrostatic equilibrium; see Hauschildt *et al.* (2003). As part of this procedure, energy transport by convection is also considered. The PHOENIX code solves the equation of state, including a very large number of atoms, ions, and molecules. With respect to radiation, the one-dimensional spherically symmetrical radiative transfer equation for expanding atmospheres is solved, including a treatment of special relativity; see Hauschildt & Baron (1999). Opacities are sampled dynamically over about 80 million lines from atomic transitions and billions of molecular lines, in addition to background (i.e., continuous) opacities, to provide an emerging spectral flux as reliable and realistic as possible.

As part of our study, all spectra emergent from a stellar model atmosphere have first been calculated with a high resolution of $\Delta\lambda = 0.01 \text{ \AA}$, for a highly complete inclusion of the lines. The spectra were then binned down to a much lower resolution, which is more practical for our subsequent astrobiological analyses.

3.2. Evolution of F-type Stars

Main-sequence stars, including the Sun, represent the slowest phase of stellar evolution, since at that stage the largest energy reservoir of the star is consumed: its central hydrogen is converted to helium; see Fig. 5 for examples of F-star evolutionary tracks. All later phases, where the star becomes a red giant twice, before and after the ignition of the central helium burning, are much faster and present much larger changes in stellar luminosity; see Cuntz *et al.* (2012) for a detailed study of the implications for habitable super-Earths. Hence, as previously found, main-sequence stars are, in general, most promising in the context of astrobiology. Though there are limits, since an increasing mass accelerates stellar evolution considerably. Nonetheless, F-type stars corresponding to the mass-range of about 1.1 to 1.6 M_{\odot} , provide stable lifetimes of 2 to 4 billion years, expected to be sufficient for the origin and evolution of life.

However, regarding the evolution of effective temperatures and, in consequence, of the spectral distribution of the emergent radiation, F-type stars differ somewhat from the Sun, especially the most massive ones: Their effective temperatures rise to much higher values while still staying on the main-sequence, and there is a quick fall afterwards, and a rise again toward the end of this phase. The reason for this evolutionary behavior resides in the

cores of F-stars: while the solar core is not convective but relies purely on radiative energy transport, F-stars employ the more efficient process of convection for transporting their high amounts of produced energy to the outer layers. Inside the most massive F-stars, where core convection has gained full power, rising bubbles even overshoot the boundary set by the Schwarzschild criterion. Hence, as a by-product, the convective cores of F-stars benefit from an enhanced chemical mixing by gaining access to a larger hydrogen reservoir around them, within reach of the “overshoot length”.

Therefore, F-type stars still spend a relatively long time on the main-sequence, making good in part for their faster evolution in general. This phenomenon is most notable between 1.4 and 1.5 M_{\odot} , where overshooting sets in. However, the evolutionary behavior of F-stars after the end of central hydrogen burning also differs a bit from that of the Sun, which does neither experience overshooting nor any core convection. These particulars of stellar evolution determine both the stellar effective temperatures and luminosities (see Table 1); they also drive the changes of the spectral characteristics of the irradiation and, finally, the inner and outer limit of the respective habitable zones.

Compared to G-type and K-type stars, F-type stars move relatively fast through the final stages of evolution beyond the main-sequence. In those stages, very dramatic changes in luminosity (increasing by over a factor 10^3), stellar radius (increasing by over a factor 100) and effective temperature (decreasing by over a factor 2) occur. The corresponding time scales are limited to a few hundred million years compared to the Sun, which will take about 2 billion years for completing these steps. For these reasons, we will restrict the study of circumstellar habitability of F-stars to their phases on and near the main-sequence.

3.3. Evolution of F-star Climatological Habitable Zones

Next we focus on the evolution of F-star climatological habitable zones, and the subsequent identification of the inner and outer limits of the CHZs and GHZs. As pointed out in Sect. 3.2, F-type stars, alike the Sun, encounter a slow but consistent growth of luminosity during their main-sequence phase as well as characteristic changes of the stellar effective temperatures. This is relevant for all types of F-stars, i.e., for the entire range of masses between about 1.2 and 1.5 M_{\odot} as addressed in the following. These masses are identified as such at the zero-age main-sequence (ZAMS), and they experience little change prior to the departure of the star toward the red giant domain; the latter is outside the scope of this study.

An example is given as Figure 6. It shows the evolution of the climatological habitable

zone for a star with an initial mass of $1.3 M_{\odot}$. It also depicts the development of the Earth-equivalent position³ given as $\sqrt{L_*}$ (with L_* as stellar luminosity in solar units), which is progressively moving outward. Note that by the end of central hydrogen burning, the total stellar radiation output has almost doubled, entailing a considerable increase of both the inner and outer limits of the climatological habitable zone, identified either as CHZ or GHZ. Furthermore, the stellar spectral types change due to alterations of their effective temperatures during the course of stellar evolution, including main-sequence evolution. In the latter case, stars of initial masses between 1.2 and $1.5 M_{\odot}$ stay within the F-type range (see Table 2).

Although it is appropriate to explore UV-based habitability at any distance from a planetary host star, we rather select the inner and outer limits of the CHZ (labelled as iC and oC, respectively), and the inner and outer limits of the GHZ (labelled as iG and oG, respectively) as venues of our study. Results are given in Table 3 and Figure 7. We especially consider the extreme positions of the iG, iC, oC, and oG attained as consequence of the stellar main-sequence evolution, i.e., as identified at the ZAMS stage and when the stars depart from the main-sequence. Our study indicates once again that when stars age the climatological habitable zones become broader and migrate outwardly.

A special aspect of significance to astrobiology concerns the continuous domains of both the CHZs and GHZs, also referred to as continuously habitable zones (see Fig. 7), where the criteria for the CHZs and GHZs (see Sect. 2.1) are fulfilled for a distinct period of time (here: the stellar main-sequence stages). The continuously habitable zones have evidently much smaller widths than the habitable zones defined by the extremes for the same amounts of time. The continuous domains of habitability for our set of stars are particularly small for the CHZs. For a $1.2 M_{\odot}$ this domain extents from 1.366 to 1.688 AU, whereas for a $1.5 M_{\odot}$ it extents only from 2.535 to 2.566 AU; this aspect should be taken into account for any comprehensive habitability assessment.

³ A more technical definition of an Earth-equivalent position involves an interpolation between the inner and outer limits of the CHZ. In this case, it depends both on the stellar luminosity and effective temperature; see, e.g., Selsis *et al.* (2007) and Cuntz (2014) for details.

4. Results and Discussion

4.1. Stellar Case Studies

The aim of our study is the investigation of biological damage inflicted upon DNA due to stellar UV radiation for objects around main-sequence F-type stars. Our results will be given in terms of E_{eff} , a parameter defined as the ratio of damage for a given distance from the star for an object with or without atmospheric attenuation relative to the damage for an object at 1 AU from a solar-like star without atmospheric attenuation present. We will focus on the following aspects: (1) influence of spectral types of the host stars, especially for F0 V, F2 V, F5 V, and F8 V, (2) relevance of planetary positions in the stellar habitable zones, including the general and conservative inner limits, Earth-equivalent positions, and the general and conservative outer limits, (3) effects of planetary atmospheric attenuation approximated by analytic functions, and (4) the relative importance of UV-A, UV-B, and UV-C regarding the DNA damage.

The DNA damage in the habitable zones around F0 V, F2 V, F5 V, and F8 V stars in cases without planetary atmospheric attenuation is found to be almost always more significant than for the reference object at Earth distance from a solar-like star (see Figure 8). The sole exception is for objects at the outer limit of the GHZ around an F8 V star, which in the solar system would correspond to an orbit beyond Mars; here E_{eff} is given as 0.95. Planetary atmospheric attenuation effectively reduces the damage of DNA, as expected (see Figure 9). In this work, as a standard example adopted for tutorial reasons, the planetary attenuation parameters are chosen as $A = 0.05$, $B = 300$, and $C = 0.5$, except otherwise noted. In this case of attenuation, the damage on DNA, for positions at the inner limit of the GHZs, is drastically reduced compared to the reference object without any attenuation. For other positions in the stellar habitable zones, the reductions are relatively high as well (see Figure 9).

It is particularly intriguing to compare the respective values of E_{eff} for F0 V, F2 V, F5 V, and F8 V stars for different positions in the stellar habitable zones as they indicate the role of the significantly higher UV fluxes of F-type stars compared to the photospheric radiation of a solar-like star. For the inner limits of the GHZs (i.e., the closest positions to the stars considered), E_{eff} for F0 V, F2 V, F5 V, and F8 V stars are identified as 9.8, 7.3, 4.2, and 3.6 without atmospheric attenuation; they decrease to 0.23, 0.19, 0.14, and 0.14, respectively, when our default choice of atmospheric attenuation is applied. At Earth-equivalent positions (which depend on the stellar spectral type much like the above-mentioned limits of habitability), E_{eff} for each star are given as 7.1, 5.2, 3.0, and 2.5, respectively, without atmospheric attenuation, and as 0.16, 0.14, 0.10, 0.10 with attenuation. At the outer limits

of GHZs, E_{eff} for each star is given as 2.9, 2.1, 1.1, and 0.95 without atmospheric attenuation, and as 0.067, 0.055, 0.038, and 0.037 with attenuation. Intermediate values are obtained for the inner and outer limits of the CHZs.

In all cases DNA damage due to UV-A, compared to UV-B and UV-C, is minuscule at best. E_{eff} due to UV-A at the inner limit of the GHZ for an F0 V star is 2.46×10^{-5} without atmospheric attenuation, which is the maximum value of all cases considered. This value is further reduced to 1.13×10^{-5} in case of default atmospheric attenuation. Of the three regimes of UV, the one most affected by our above choice of planetary attenuation is UV-C. For F0 V, F2 V, F5 V, and F8 V, the DNA damage due to UV-C is 96%, 95%, 93%, and 91%, respectively, of the total for the UV regimes combined. If atmospheric attenuation is included, the DNA damage due to UV-C is reduced to 1.7%, 1.9%, 2.3%, and 2.6% of the damage due to UV-C without planetary attenuation. It comprises 70%, 68%, 65%, and 61% of the total for each case of attenuation. The relative damage attributable to UV-C decreases with stellar types from F0 V to F8 V. The damage due to UV-A and UV-B also decreases with stellar types from F0 V to F5 V, but it slightly increases between F5 V and F8 V because of the shape of the stellar photospheric spectrum (see Figure 5).

4.2. Impact of Planetary Atmospheric Attenuation

Since atmospheric attenuation is expected to impact preferably the UV regime, which in turn is most relevant to the DNA damage, we also explored the effects of parameter choices for the attenuation function ATT (see Eq. 3). For tutorial reasons, we focused on the F2 V star, and varied one of the parameters, i.e., A , B , or C , at a time. Figure 10 depicts two cases out of several combinations of fixed parameters that were investigated. In the top panels of Figure 10, the parameter A is varied from 0.01 to 1.0, whereas the other parameters remain fixed at $B = 300$ and $C = 0.5$. In the bottom panels, the parameter B is varied from 250 to 350 and the two other parameters remain fixed at $A = 0.05$ and $C = 0.5$. The two panels on the left show the relative impact of UV-A, UV-B, and UV-C on DNA at an Earth-equivalent position. Note that the impact of UV-A is, however, completely unrecognizable in all panels. The two panels to the right show the DNA damage at five selected positions in the habitable zone of the F2 V star, which are: the inner limits of the GHZs and CHZs, the Earth-equivalent position, and the outer limits of the CHZs and GHZs. It is found that damage inflicted on DNA is considerably larger for objects closer to the star. Thus, in Fig. 10, the top two lines represent the inner limits of the CHZ and GHZ, and the bottom two lines represent the outer limits of the CHZ and GHZ.

The parameter A depicts the rate of change in ATT with increasing wavelength (see

Fig. 3). Thus, a smaller value of A corresponds to a gentler slope of ATT, but also to a considerably higher value of ATT at relatively short wavelength (i.e., near 200 nm), which implies a higher effect of attenuation where damage inflicted on DNA is most severe (see Fig. 2). The parameter B describes the center wavelength of the attenuation function; it also changes the response of each regime to varied values of A . Thus, the appearance of E_{eff} as function of the attenuation parameter A heavily depends on the fixed value of parameter B . For example, let us consider the case $B = 300$. Here, the DNA damage due to UV-A increases, while the damages due to UV-B and UV-C decrease as the parameter A increases (see Fig. 10). Here E_{eff} decreases from 0.73 to 0.0074 for an Earth-equivalent position with increasing A . The largest changes occur between $A = 0.01$ and 0.08, where E_{eff} due to UV-C declines drastically. In these cases, especially for our standard choice of attenuation (see Sect. 4.1), most of the DNA damage is attributable to UV-C. But for $A = 0.08$, E_{eff} due to UV-B and due to UV-C are about the same, and for larger values of A , E_{eff} due to UV-B becomes greater than E_{eff} due to UV-C.

We also varied the parameter B while keeping the values for A and C fixed. E_{eff} is identified as a decreasing function for variable values of B . Since parameter B determines the center of the attenuation function, the effect of UV diminishes from the lowest wavelengths as B is increased. In other words, UV-C is affected the most by varying B . If $A = 0.05$ and $C = 0.5$ are used, E_{eff} decreases from 1.32 at $B = 250$ to 0.14 at $B = 300$ and to 0.0012 at $B = 350$ for objects at Earth-equivalent positions. This behavior is shown in Figure 10. If $A = 0.1$ and $C = 0.5$ are used, the appearance of each functional dependence is similar to the case of $A = 0.05$; however, E_{eff} of UV-B exceeds that of UV-C at $B = 293$. The functional dependence for UV-C is steeper for $A = 0.1$ than for $A = 0.05$. The total amount of E_{eff} decreases from 1.36 at $B = 250$ to 0.048 at $B = 300$ and to 3.9×10^{-6} at $B = 350$ for objects at the Earth-equivalent position.

DNA damage is inversely proportional to the square of distance between a planet and the host star, and thus, the ratio of DNA damage (with or without the consideration of atmospheric attenuation) at one position to another does not change with the selected combination of parameters. Because of that, if E_{eff} , the ratio of DNA damage at a position to the reference value, at different positions are compared, the differences are smaller for more effective combinations of parameters. For example, the DNA damage at the inner limits of the GHZs and the CHZs, and at the outer limits of the CHZs and GHZs are 139%, 108%, 62%, and 40% of DNA damage as measured by E_{eff} , respectively, as found for the F2 V star. If attenuation is considered, and if the attenuation parameters are chosen as $(A, B, C) = (0.01, 300, 0.5)$, E_{eff} is found as 1.01, 0.78, 0.73, 0.45, and 0.29 at the inner limit of the GHZ and CHZ, at the Earth-equivalent position, and at the outer limit of the CHZ and GHZ, respectively. By contrast, if the same parameters are set as $(A, B, C) = (0.5, 300, 0.5)$, our standard choice),

E_{eff} is identified as 0.0119, 0.0092, 0.0086, 0.0053 and 0.0034, respectively.

4.3. Habitability during the Course of F-Star Evolution

We also studied the influence of stellar main-sequence evolution, resulting in pronounced changes in the stellar effective temperatures and luminosities regarding the damage inflicted on DNA. Again, we consider cases without and with planetary atmospheric attenuation (see Sect. 4.1). Specifically, we explore the change in E_{eff} at specific positions in the habitable zones for stars with masses of 1.2, 1.3, 1.4, and 1.5 M_{\odot} . The selected positions are the general outer limit at ZAMS (bottom dotted line in Figures 11 and 12), the conservative outer limit at ZAMS (bottom dashed line), the general inner limit at the end of main-sequence (top dotted line), the conservative inner limit at the end of main-sequence (top dashed line), the Earth-equivalent positions at ZAMS (i.e., minimum distance; top solid line) and the end of main-sequence (i.e., maximum distance value; bottom solid line); see Sect. 3.3. The distances for various positions are given in Table 4 and Figure 7.

Furthermore, we also consider average (i.e., time-independent) Earth-equivalent positions, which are derived by interpolating the conservative outer limit at the ZAMS and the conservative inner limit at the end of main-sequence evolution noting that these limits correspond to the continuous domains of the CHZs. Generally, the Earth-equivalent positions are computed as weighted averages between the inner and outer limits of the CHZs, which can be approximated as $0.95\sqrt{L_*}$ and $1.37\sqrt{L_*}$ (with L_* in solar units), respectively, with the Earth-equivalent positions given as $\sqrt{L_*}$ (Kasting *et al.* 1993). For stars with masses of 1.2, 1.3, 1.4, and 1.5 M_{\odot} , the average Earth-equivalent positions are obtained as 1.56, 1.82, 2.10, and 2.54 AU, respectively, which in the Solar System would correspond to an approximate distance nearly between Mars and Ceres. Moreover, we also consider evolving Earth-equivalent positions, noting that the inner and outer limits of CHZs change on evolutionary time scales (see Fig. 7); see discussion below.

In principle, the damage inflicted on DNA at any position within the stellar habitable zones at the ZAMS increases as a function of the stellar mass (see Figures 11 and 12). Regarding the inner and outer limits of both the CHZs and GHZs, the damage on DNA first increases with evolutionary time, but then starts decreasing with time, while the stellar luminosity keeps increasing and both the CHZs and GHZs continue to migrate outward. If no planetary attenuation is considered, the ZAMS E_{eff} values at average Earth-equivalent positions for stars of 1.2, 1.3, 1.4, and 1.5 M_{\odot} are found as 0.91, 2.46, 3.41, and 5.02, respectively. The maximum values for the DNA damage, expressed as E_{eff} , at average Earth-equivalent positions are given as 1.96, 2.63, 3.48, and 5.07, respectively. These values

are obtained at stellar evolutionary times of 1.95, 0.93, 0.27, and 0.14 Gyr, respectively; it means that the maximum amounts of damage inflicted on DNA are attained much earlier for stars of higher mass (and, by implication, of earlier spectral type and higher initial effective temperature). At the end of main-sequence evolution, the E_{eff} values at average Earth-equivalent positions are then reduced to 0.96, 1.04, 1.07, and 0.32, respectively; they are comparable to or smaller than those for a reference object orbiting a solar-like star.

If default planetary atmospheric attenuation is assumed, corresponding to $(A, B, C) = (0.05, 300, 0.5)$, the damage is drastically reduced, i.e., by up to 96%, 97%, 97%, and 98% for stars of 1.2, 1.3, 1.4, and 1.5 M_{\odot} , respectively. The precise amount of reduction is a function of the stellar evolutionary status. The amount of reduction moreover depends on the type of star, which determines the shape of the emergent spectrum, therefore entailing different amounts of damage. As previously discussed, the damage is dominated by the UV-C regime (see Eq. 1 and Fig. 2). If standard attenuation is considered, the ZAMS values for E_{eff} at average Earth-equivalent positions for stars of 1.2, 1.3, 1.4, and 1.5 M_{\odot} are reduced to 0.038, 0.082, 0.098, and 0.121, respectively. The maximum E_{eff} values at those positions are given as 0.075, 0.087, 0.099, and 0.122, whereas at the end of the main-sequence stages, they are further reduced to 0.040, 0.041, 0.041, and 0.014, respectively.

For specific age intervals, E_{eff} changes in different ways in the vicinities of stars of different masses. The following data refer to objects at average Earth-equivalent positions, but they can also be converted for other star–planet distances in a highly straightforward manner. We are particularly interested in the change of E_{eff} between 0.5 Gyr and 2.5 Gyr, i.e., during the early stages of the systems, contemporaneous with the time when life originated on Earth (e.g., Brack 1998, and references therein), For a star with masses of 1.2 M_{\odot} , E_{eff} increases from 1.75 to 1.96 until 1.95 Gyr, and thereafter decreases to 1.92 at the average Earth-equivalent position if planetary atmospheric attenuation is absent. For a star with masses of 1.3 M_{\odot} , E_{eff} increases from 2.61 to 2.63 until 0.93 Gyr, and then decreases to 1.86. For stars with masses of 1.4 M_{\odot} and 1.5 M_{\odot} , E_{eff} decreases from 3.46 to 1.10 and decreases from 4.88 to 0.52, respectively. Thus, a planet in the habitable zone of a 1.2 M_{\odot} mass star will experience the least change in the amount of DNA damage, whereas that change will be greatest for a 1.5 M_{\odot} mass star.

Adequate models should also take into account effects due to planetary atmospheric attenuation. In this case, even the climatological habitable zone of a 1.5 M_{\odot} mass star may be able to offer a relatively well UV protected environment throughout the early 2 Gyr period. The same statement is expected to apply for F-type stars of lower mass as well. If our default model of atmospheric attenuation is adopted, E_{eff} for a 1.2 M_{\odot} mass star increases from 0.069 to 0.075 until 1.95 Gyr, and then decreases to 0.074; note that these data refer

to average Earth-equivalent positions. For a $1.3 M_{\odot}$ mass star, E_{eff} for the same setting increases from 0.086 to 0.087 until 0.93 Gyr, and then decreases to 0.067. In comparison, for stars with masses of 1.4 and $1.5 M_{\odot}$, E_{eff} decreases from the maximum value of 0.099 to 0.042 and from 0.118 to 0.021, respectively. For other planetary positions, the respective values for E_{eff} can be obtained through appropriate scaling.

Moreover, we also computed the DNA damage at evolving (i.e., time-dependent) Earth-equivalent positions, depicted as dashed lines in Fig. 7. For all cases from 1.2 to $1.5 M_{\odot}$, the Earth-equivalent positions at ZAMS are located very close to the stars. In fact, they are situated interior to the continuous domains of both the CHZs and GHZs. As the stars age, the Earth-equivalent positions migrate outward, crossing or even passing the continuous domains of the CHZs, especially for relatively massive F-type stars. Since the damage inflicted on DNA is proportional to the square of distance from the star, the attained results reflect the behavior of the planetary positions. The maximum DNA damage at evolving Earth-equivalent positions without atmospheric attenuation for stars of 1.2, 1.3, 1.4, and $1.5 M_{\odot}$ are given as 2.55, 3.56, 4.74, and 7.74, respectively, occurring at very early stages of the stellar lifetimes, whereas the minimum DNA damage are given as 0.92, 0.99, 1.01, and 0.29, respectively, obtained at the end of main-sequence evolution (see Fig. 11). Damage on DNA is reduced by planetary atmospheric attenuation, as expected. For default attenuation, the maximum damage is found as 0.099, 0.119, 0.136, and 0.186, respectively, whereas the minimum damage is found as 0.038, 0.040, 0.039, and 0.012, respectively (see Fig. 12).

5. Summary and Conclusions

In this study, we investigated the general astrobiological significance of F-type main-sequence stars. DNA has been taken as a proxy for carbon-based macromolecules following the paradigm that extraterrestrial biology may most likely be associated with hydrocarbon-based biochemistry. Consequently, the DNA action spectrum was utilized to describe the impact of the stellar UV radiation. We considered an array of important aspects, including (1) the role of stellar main-sequence evolution, (2) the situation for planets at different positions within the stellar habitable zones, and (3) the general influence of planetary atmospheric attenuation, which has been described based on a parameterized attenuation function. The damage on DNA was described by the output parameter E_{eff} , defined as the ratio of damage for a given distance from the star for a general object relative to the damage for an object at 1 AU from a solar-like star with attenuation absent.

We found the following results:

(1) For average Earth-equivalent planetary positions, located inside the continuous domains of the CHZs, E_{eff} for stars of spectral type F0 V, F2 V, F5 V, and F8 V are obtained as 7.1, 5.2, 3.0, and 2.5, respectively. Earth-equivalent planetary positions depend on the stellar spectral type, and are at greater distance for stars of higher effective temperature or, by implication, larger mass. These results are consistent with the earlier work by Cockell (1999).

(2) For the inner and outer limits of the CHZs as well as GHZs, the results for E_{eff} can be obtained by scaling. Specifically, the damage inflicted on DNA is considerably increased at the inner limits of the CHZs and GHZs and considerably decreased at the outer limits of the CHZs and GHZs relative to average Earth-equivalent positions. For F2 V stars, the scaling factors for the inner limits are given as 139% and 108% and for the outer limits as 62% and 40% relative to that at average Earth-equivalent positions.

(3) Owing to the form of the DNA action spectrum (see Fig. 2), in the absence of significant planetary atmospheric attenuation, most of the damage on DNA is because of UV-C. Damage due to UV-B is significantly lower, and damage due to UV-A is virtually nonexistent. Regarding the latter, the largest value in the context of this study was attained at the inner limit of the GHZ for an F0 V star in the absence of planetary atmospheric attenuation, which is 2.46×10^{-5} .

(4) Planetary atmospheric attenuation, especially that associated with ozone layers (e.g., Segura *et al.* 2003), is able to reduce damage inflicted on DNA drastically. In consideration of realistic atmospheric attenuation functions, this aspect entails a drastic reduction of damage associated with UV-C. On a relative scale, it thus tends to increase the importance of UV-B.

(5) It is particularly intriguing to assess the behavior of E_{eff} during stellar main-sequence evolution, which has been evaluated in detail for stars of masses of 1.2, 1.3, 1.4, and 1.5 M_{\odot} . If no planetary attenuation is taken into account, the ZAMS E_{eff} values at average Earth-equivalent positions are identified as 0.91, 2.46, 3.41, and 5.02, respectively. The E_{eff} values at other positions in the stellar habitable zones can be obtained by scaling noting that the incident stellar radiation is diluted following the inverse square law.

(6) Taking average Earth-equivalent positions as reference, the E_{eff} values are found to change with time in response to changes in the stellar parameters owing to the stellar main-sequence evolution. E_{eff} first increases with time and reach maximum values of 1.96, 2.63, 3.48, and 5.07 for stars with masses of 1.2, 1.3, 1.4, and 1.5 M_{\odot} , respectively; they are attained at evolutionary times of 1.95, 0.93, 0.27, and 0.14 Gyr, respectively. Thereafter, the E_{eff} values decline. They reach 0.96, 1.04, 1.07, and 0.32 for the selected set of stars. These values are comparable to or smaller than that at an Earth-equivalent position for a solar-like star.

Our study is a further contribution toward the exploration of the exobiological suitability of stars hotter and, by implication, more massive than the Sun. Although these stars are relatively rare compared to G-type solar-type stars, they possess significantly augmented habitable zones. On the other hand, their emergent photospheric UV fluxes are much larger; fortunately, however, they can be diminished through planetary atmospheric attenuation. Thus, at least in the outer portions of F-star habitable zones, UV radiation should not be viewed as an insurmountable hindrance to the existence and evolution of life. Future studies for F-type stars should encompass (1) detailed chemical models of planetary atmospheres, aimed at constraining the attenuation parameters, (2) examples of specific star–planet systems with information attained from observational constraints, and (3) cases of F-type stars that are members of binary (or higher order) systems. Studies of the circumstellar habitability for those systems also encompassing analyses of planetary orbital stability have been given by, e.g., Cuntz (2014) and others.

Acknowledgements. This work has been supported by the Department of Physics, University of Texas at Arlington (S. S., M. C.), by a UGTO/PROMEP-funded project (D. J.), and by a CONACyT master student stipend (C. M. G. O.). Additionally, K. P. S. is grateful for CONACyT support of his sabbatical year projects under application No. 207662.

REFERENCES

- Brack, A. (1998). (Ed.) *The Molecular Origins of Life: Assembling Pieces of the Puzzle*. Cambridge Univ. Press, Cambridge.
- Buccino, A.P., Lemarchand, G.A. & Mauas, P.J.D. (2006). *Icarus* **183**, 491–503.
- Chabrier, G. (2003). *Publ. Astron. Soc. Pac.* **115**, 763–795.
- Cockell, C.S. (1998). *J. Theor. Biol.* **193**, 717–729.
- Cockell, C.S. (1999). *Icarus* **141**, 399–407.
- Cockell, C.S. (2002). In *Astrobiology: The Quest for the Conditions of Life*, ed. Horneck, G. and Baumstark-Khan, C., pp. 219–232. Springer, Berlin.
- Cuntz, M., von Bloh, W., Schröder, K.-P., Bounama, C. & Franck, S. (2012). *Int. J. Astrobiol.* **11**, 15–23.
- Cuntz, M. (2014). *Astrophys. J.* **780**, 14 (19 pp.).
- Diffey, B.L. (1991). *Physics in Medicine and Biology* **36**, 299–328.
- Forget, F. & Pierrehumbert, R.T. (1997). *Science* **278**, 1273–1276.
- Grenfell, J.L., Stracke, B., von Paris, P., Patzer, B., Titz, R., Segura, A. & Rauer, H. (2007). *Pla. Space Sci.* **55**, 661–671.
- Güdel, M. (2007). *Living Rev. Sol. Phys.* **4**, 3 (137 pp.).
- Guinan, E.F. & Ribas, I. (2002). In *The Evolving Sun and Its Influence on Planetary Environments*, Proc. ASP Conf. Ser. 269, ed. Montesinos, B., Gimenez, A. and Guinan, E.F., pp. 85–106. Astr. Soc. Pac., San Francisco.
- Hauschildt, P.H. (1992). *J. Quant. Spectr. & Rad. Transf.* **47**, 433–453.
- Hauschildt, P.H. & Baron, E. (1999). *J. Comput. Appl. Math.* **109**, 41–63.
- Hauschildt, P.H., Allard, F. & Baron, E. (1999). *Astrophys. J.* **512**, 377–385.
- Hauschildt, P.H., Barman, T.S., Baron, E. & Allard, F. (2003). In *Stellar Atmosphere Modeling*, ed. Hubeny, I., Mihalas, D. and Werner, K., pp. 227–238. ASP Conf. Ser. 288, San Francisco.
- Henderson, S.T. (1977). *Daylight and Its Spectrum.*, 2nd edn. Wiley, New York (349 pp.).

- Horneck, G. (1995). *J. Photochem. Photobiol. B: Biology* **31**, 43–49.
- Horner, J. & Jones, B.W. (2010). *Int. J. Astrobiol.* **9**, 273–291.
- Jones, B.W., Underwood, D.R. & Sleep, P.N. (2005). *Astrophys. J.* **622**, 1091–1101.
- Jones, B.W., Sleep, P.N. & Underwood, D.R. (2006). *Astrophys. J.* **649**, 1010–1019.
- Jones, B.W. (2008). *Int. J. Astrobiol.* **7**, 279–292.
- Kasting, J.F., Whitmire, D.P. & Reynolds, R.T. (1993). *Icarus* **101**, 108–128.
- Kaltenegger, L., Eiroa, C., Ribas, I., Paresce, F., Leitzinger, M., Odert, P., Hanslmeier, A., Fridlund, M., Lammer, H., Beichman, C., *et al.* (2010). *Astrobiology* **10**, 103–112.
- Kaltenegger, L., Miguel, Y. & Rugheimer, S. (2012). *Int. J. Astrobiol.* **11**, 297–307.
- Kroupa, P. (2002). *Science* **295** (5552), 82–91.
- Kudritzki, R.-P. & Puls, J. (2000). *Ann. Rev. Astron. Astrophys.* **38**, 613–666.
- Lammer, H. (2007). *Astrobiology* **7**, 27–29.
- Lammer, H., Selsis, F., Ribas, I., Guinan, E.F., Bauer, S.J. & Weiss, W.W. (2003). *Astrophys. J. Lett.* **598**, L121–124.
- Lammer, H., Bredehöft, J.H., Coustenis, A., Khodachenko, M.L., Kaltenegger, L., Grasset, O., Prieur, D., Raulin, F., Ehrenfreund, P., Yamauchi, M. *et al.* (2009). *Astron. Astrophys. Rev.* **17**, 181–249.
- Lammer, H., Blanc, M., Benz, W., Fridlund, M., du Foresto, V.C., Güdel, M., Rauer, H., Udry, S., Bonnet, R.-M., Falanga, M., *et al.* (2013). *Astrobiology* **13**, 793–813.
- Linsky, J.L. (1980). *Ann. Rev. Astron. Astrophys.* **18**, 439–488.
- Meadows, V. & Seager, S. (2011). In *Exoplanets*, ed. Seager, S., pp. 441–470. Univ. Arizona Press, Tucson.
- Maeder, A. & Meynet, G. (1988). *Astron. Astrophys. Suppl. Ser.* **76**, 411–425.
- Peak, M.J. & Peak, J.G. (1986). In *The Biological Effects of UVA Radiation*, ed. Urbach, F. and Gange, R.W., pp. 42–56. Praeger, New York.
- Pols, O.R., Tout, C.A., Eggleton, P.P. & Han, Z. (1995). *Mon. Not. R. Astron. Soc.* **274**, 964–974.

- Pols, O.R., Schröder, K.-P., Hurley, J.R., Tout, C.A. & Eggleton, P.P. (1998). *Mon. Not. R. Astron. Soc.* **298**, 525–536.
- Rettberg, P. & Rothschild, L. J. (2002). In *Astrobiology: The Quest for the Conditions of Life*, ed. Horneck, G. and Baumstark-Khan, C., pp. 233–243. Springer, Berlin.
- Scalo, J., Kaltenegger, L., Segura, A.G., Fridlund, M., Ribas, I., Kulikov, Yu.N., Grenfell, J.L., Rauer, H., Odert, P., Leitzinger, M. *et al.* (2007). *Astrobiology* **7**, 85–166.
- Schröder, K.-P. & Cuntz, M. (2005). *Astrophys. J. Lett.* **630**, L73–L76.
- Schröder, K.-P. & Cuntz, M. (2007). *Astron. Astrophys.* **465**, 593–601.
- Schröder, K.-P. & Smith, R.C. (2008). *Mon. Not. R. Astron. Soc.* **386**, 155–163.
- Schröder, K.-P., Pols, O.R. & Eggleton, P.P. (1997). *Mon. Not. R. Astron. Soc.* **285**, 696–710.
- Segura, A., Krellove, K., Kasting, J.F., Sommerlatt, D., Meadows, V., Crisp, D., Cohen, M. & Mlawer, E. (2003). *Astrobiology* **3**, 689–708.
- Selsis, F., Kasting, J.F., Levrard, B., Paillet, J., Ribas, I. & Delfosse, X. (2007). *Astron. Astrophys.* **476**, 1373–1387.
- Setlow, R.B. (1974). *Proc. Natl. Acad. Sci. USA* **71**, 3363–3366.
- Underwood, D.R., Jones, B.W. & Sleep, P.N. (2003). *Int. J. Astrobiol.* **2**, 289–299.
- Von Bloh, W., Cuntz, M., Schröder, K.-P., Bounama, C. & Franck, S. (2009). *Astrobiology* **9**, 593–602.

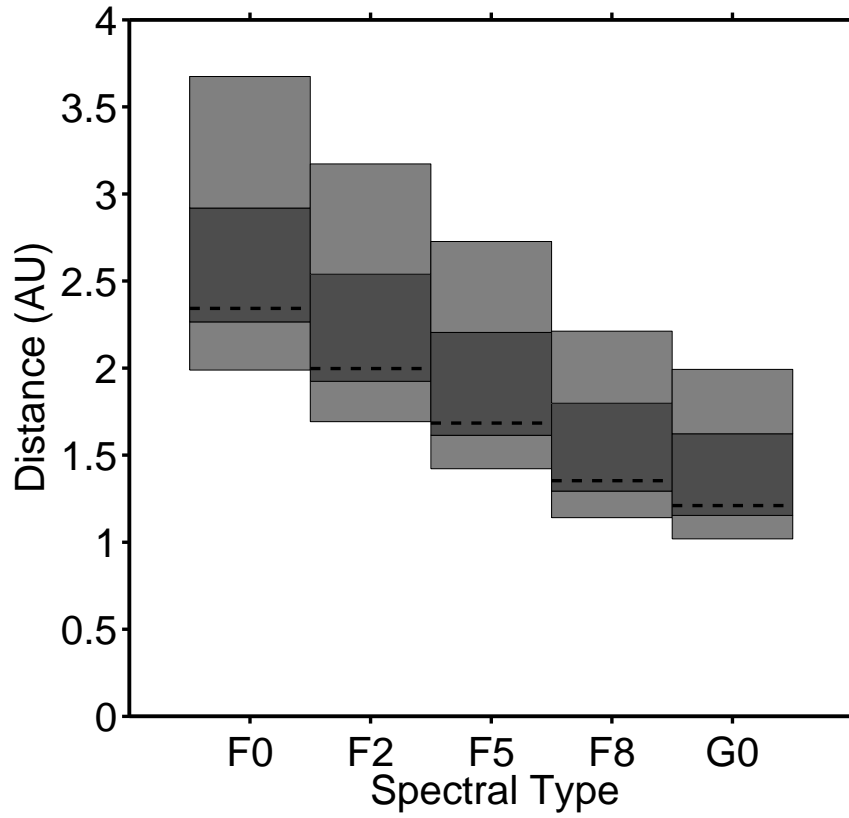


Fig. 1.— Depiction of the habitable zones for F-type stars (see Table 1 for information on the stellar parameters). Dark gray colors indicate the CHZs, whereas light gray colors indicate the GHZs. Earth-equivalent positions within the habitable zones are depicted by dashed lines.

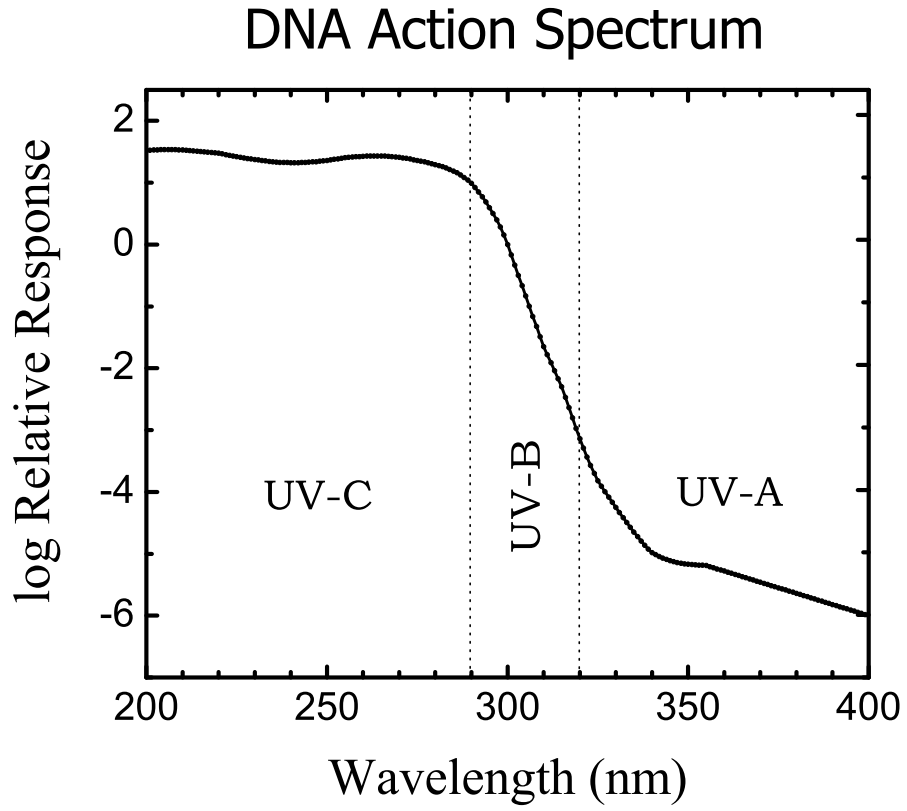


Fig. 2.— DNA action spectrum following Horneck (1995) and Cockell (1999).

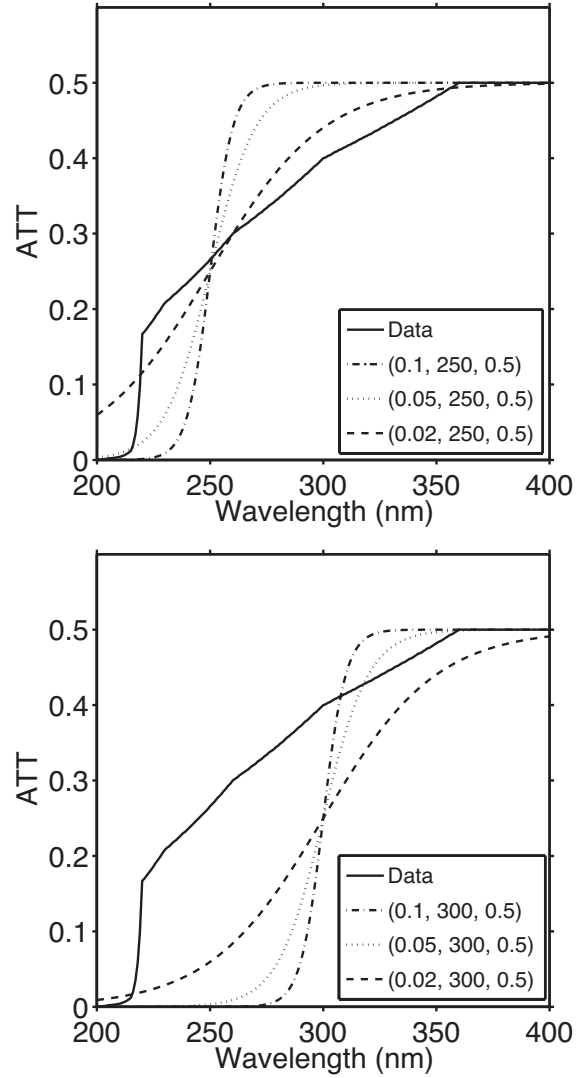


Fig. 3.— Examples of parameterized attention functions ATT defined through (A, B, C) (see Eq. 3). The solid line indicates the proposed case of Earth 3.5 Gyr ago (Cockell 2002). Note that the attention functions are not intended to fit the Earth-based data with the tentative exception of $(0.02, 250, 0.5)$.

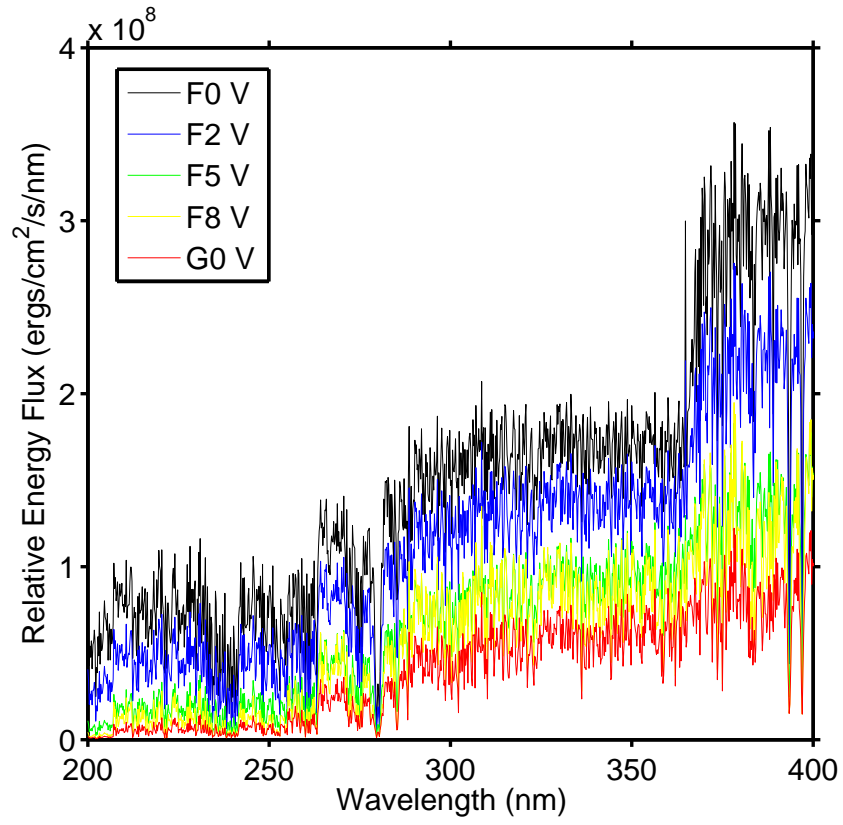


Fig. 4.— Stellar spectra as calculated by the PHOENIX code given by Hauschildt (1992) and subsequent work (see text for details).

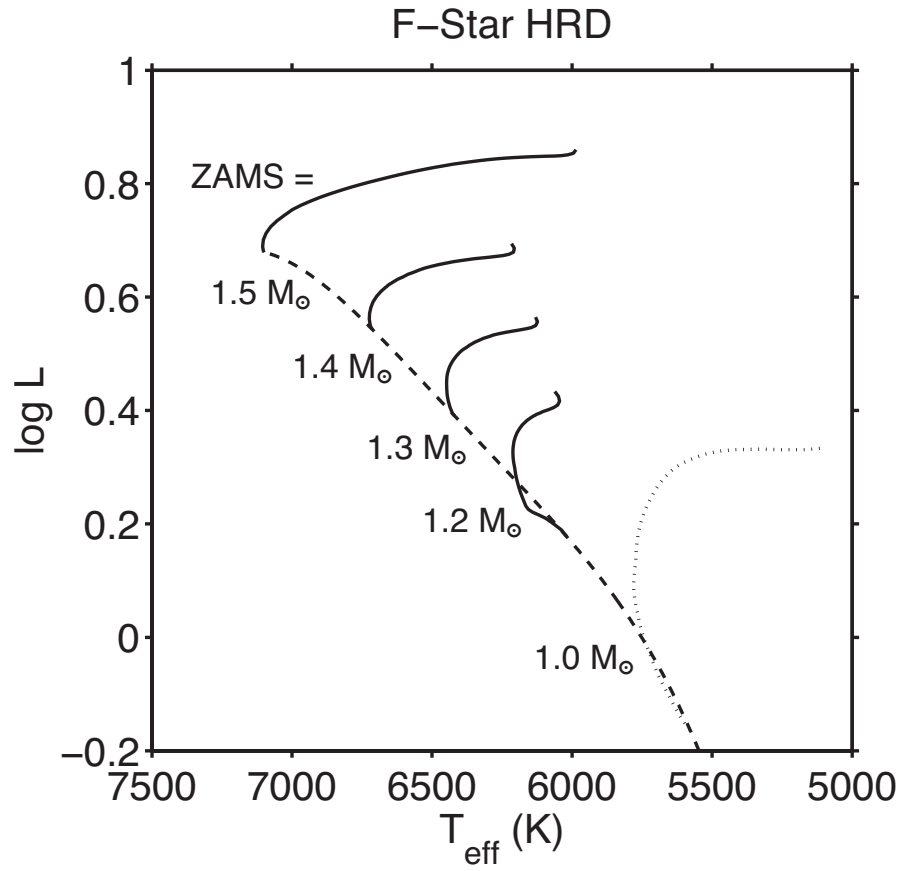


Fig. 5.— Stellar evolutionary tracks for a set of F-type stars (solid lines) denoted by their initial masses with the main-sequence depicted by a dashed line. The evolutionary track for the Sun (G2 V) is given as a dotted line.

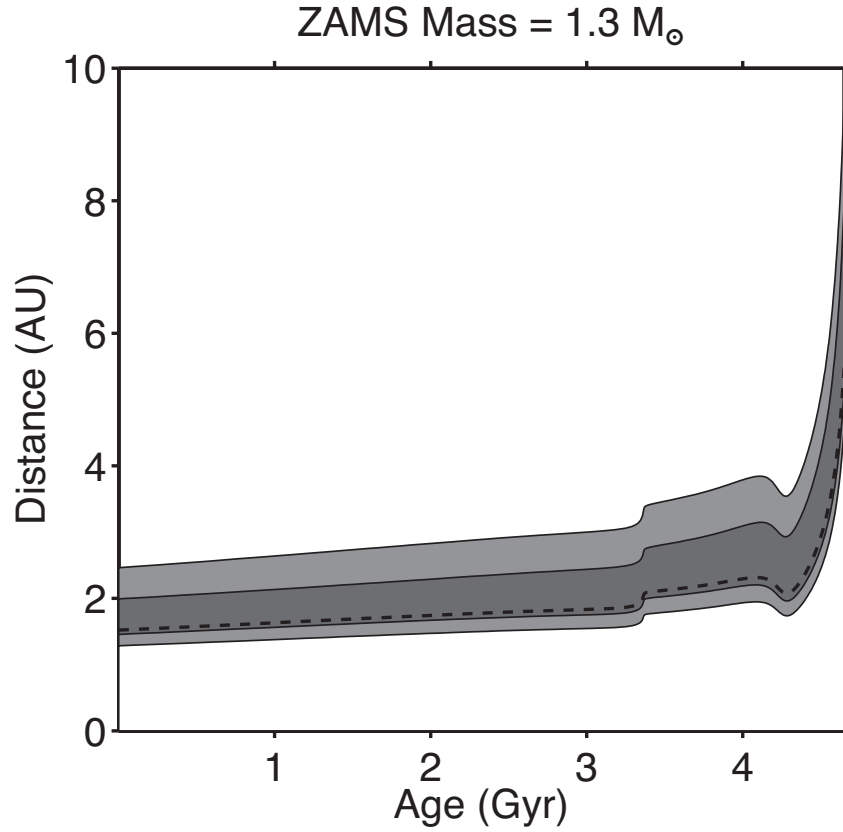


Fig. 6.— Evolution of the climatological habitable zone for a ZAMS star with a mass of $1.3 M_{\odot}$. Dark gray color indicates the CHZ, whereas light gray color indicates the GHZ. Earth-equivalent positions are depicted by a dashed line. The temporary increase of the inner and outer limits of the habitable zone, between the age of 3.5 and 4.2 billion years, reflects an episode of higher luminosity due to the onset of hydrogen shell burning.

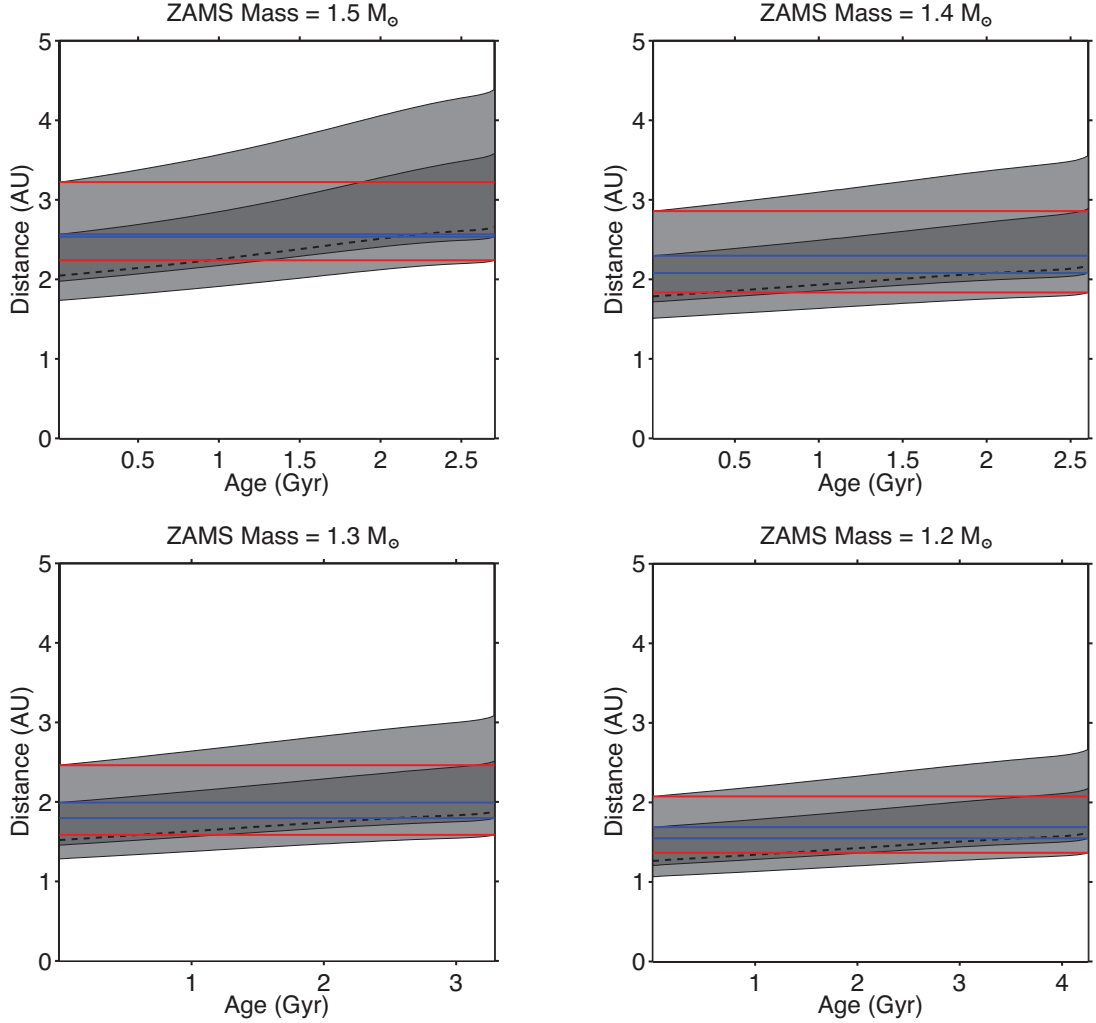


Fig. 7.— Magnified segments of the evolution of CHZs (dark gray) and GHZs (light gray) for selected F-type stars (indicated by their stellar masses) during their lifetimes on the main-sequence. The corresponding Earth-equivalent positions, which evolve with time, are depicted by dashed lines. The horizontal blue lines indicate the inner and outer limits of the continuous domains of the CHZs, whereas the horizontal red lines indicate the inner and outer limits of the continuous domains of the GHZs. Note that in the main text, we introduce an average (i.e., time-independent) Earth-equivalent position located within the CHZs obtained through interpolation between the conservative outer limit at the ZAMS and the conservative inner limit at the end of main-sequence evolution.

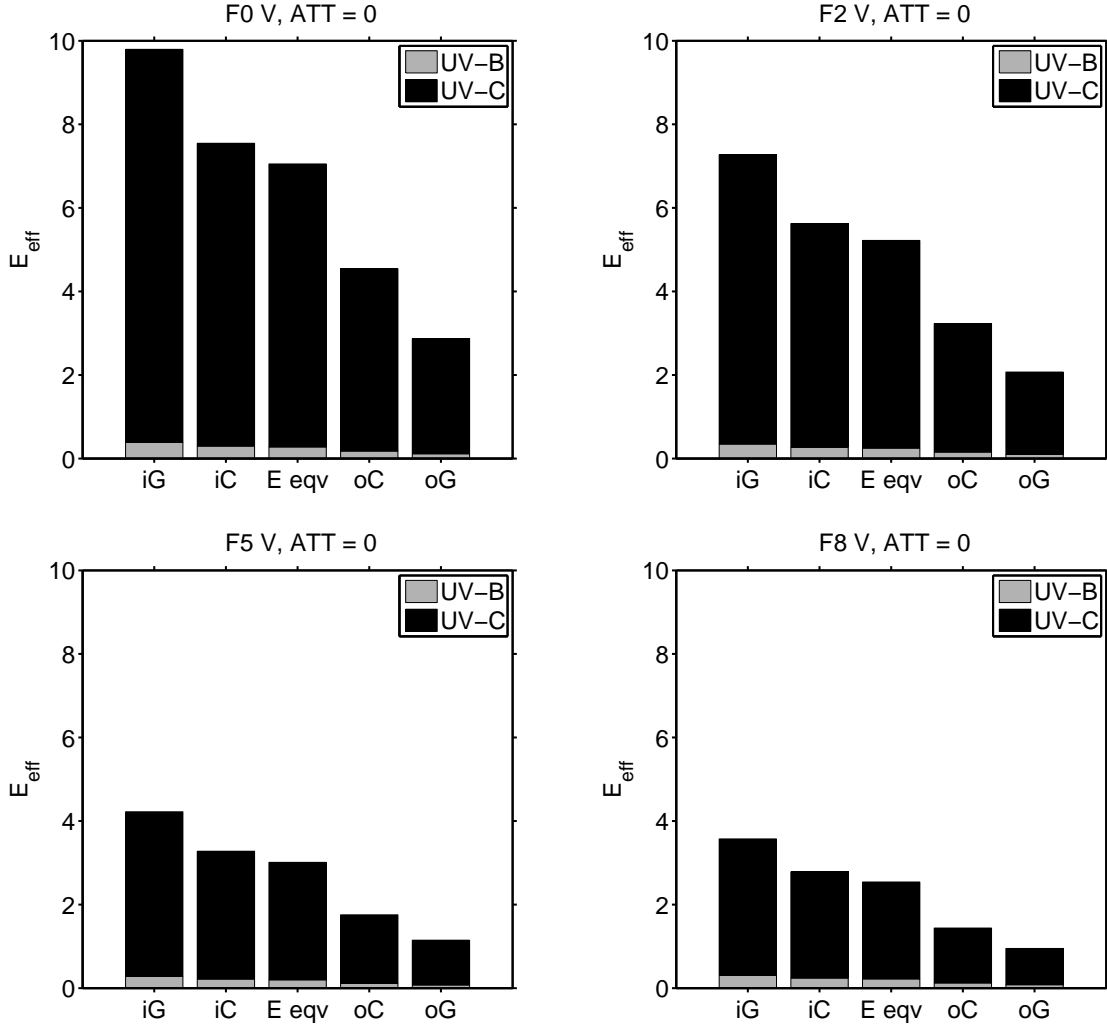


Fig. 8.— Damage due to UV-B and UV-C inflicted upon DNA (taken as a representative biomolecule) in the environments of F0 V, F2 V, F5 V, and F8 V stars determined at the inner limits of the GHZs and CHZs (iG, iC) and at the outer limits of the GHZs and CHZs (oG, oC), as well as for Earth-equivalent positions. Most of the damage occurs through UV-C, whereas minor damage occurs through UV-B. Damage associated with UV-A is unidentifiable and has therefore been omitted (see text). No planetary attenuation is taken into account (ATT=0).

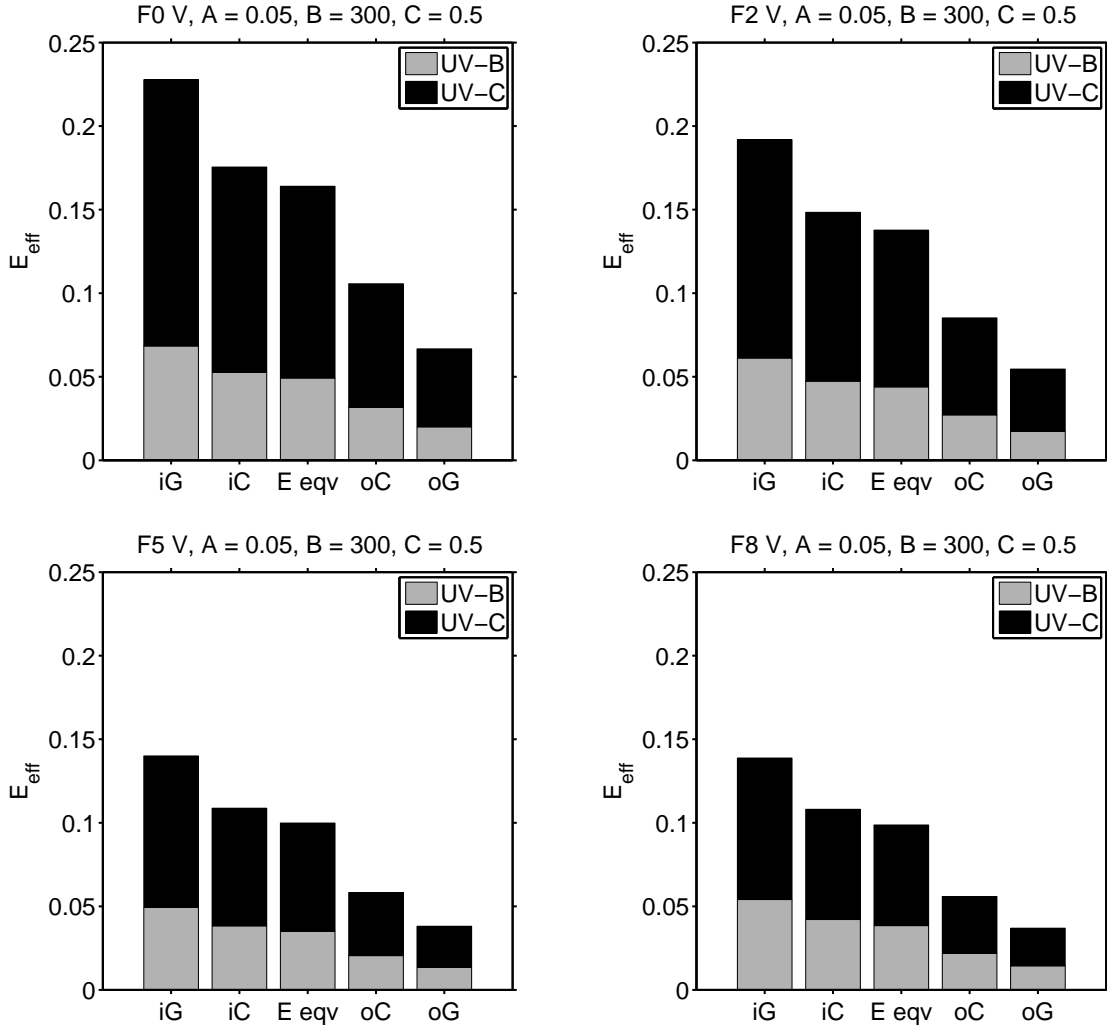


Fig. 9.— Same as Fig. 8, but with inclusion of planetary attenuation. The attenuation parameters A , B , and C are specified (see Eq. 3).

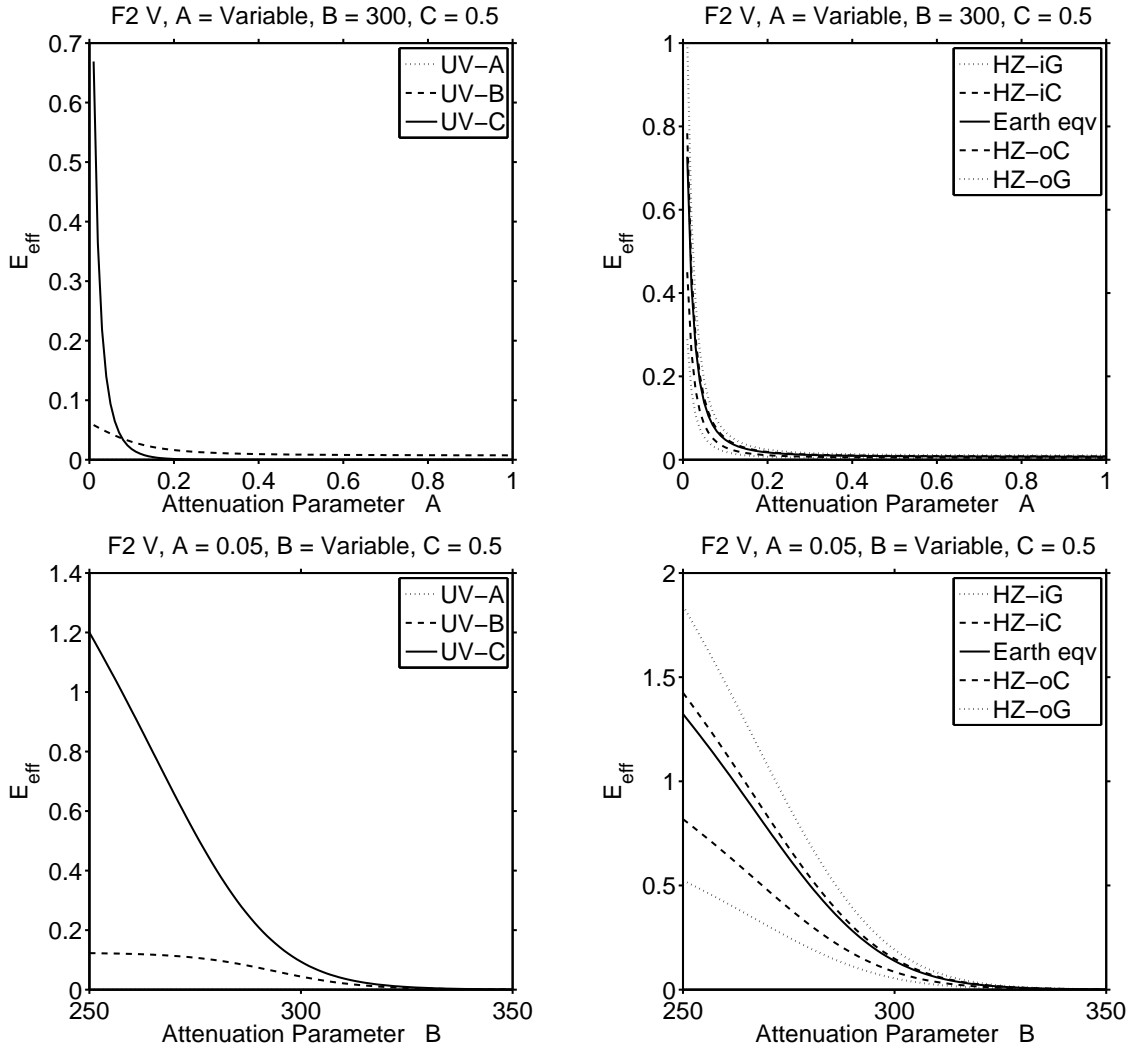


Fig. 10.— Damage inflicted upon DNA at specified positions within the habitable zone for an F2 V star. Planetary atmospheric attenuation is taken into account with parameters as specified.

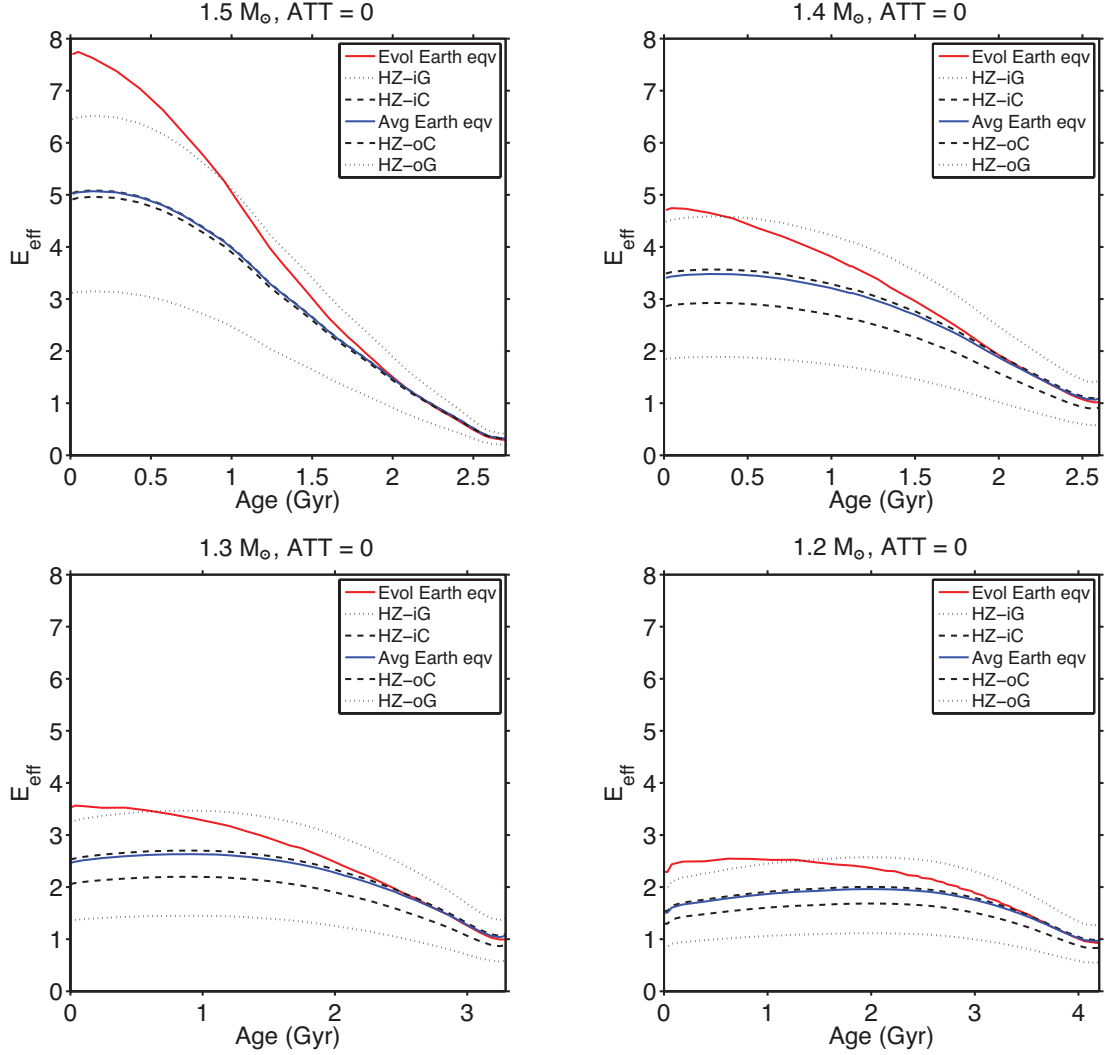


Fig. 11.— Damage inflicted upon DNA at specified positions within the habitable zone of various F-type stars, characterized by their masses, at different ages. No planetary attenuation is taken into account ($ATT=0$). Results are given for the HZ-iG, HZ-iC, HZ-oC, and HZ-oG in reference to the continuous domains of the CHZs and GHZs, respectively (see Fig. 7 and Table 4). The behaviors of the E_{eff} are largely due to the changes of the stellar luminosities. We also show the results for the average Earth-equivalent positions (embedded into the continuous domains of the CHZs) and the evolving Earth-equivalent positions. The latter conform to the dashed lines of Fig. 7.

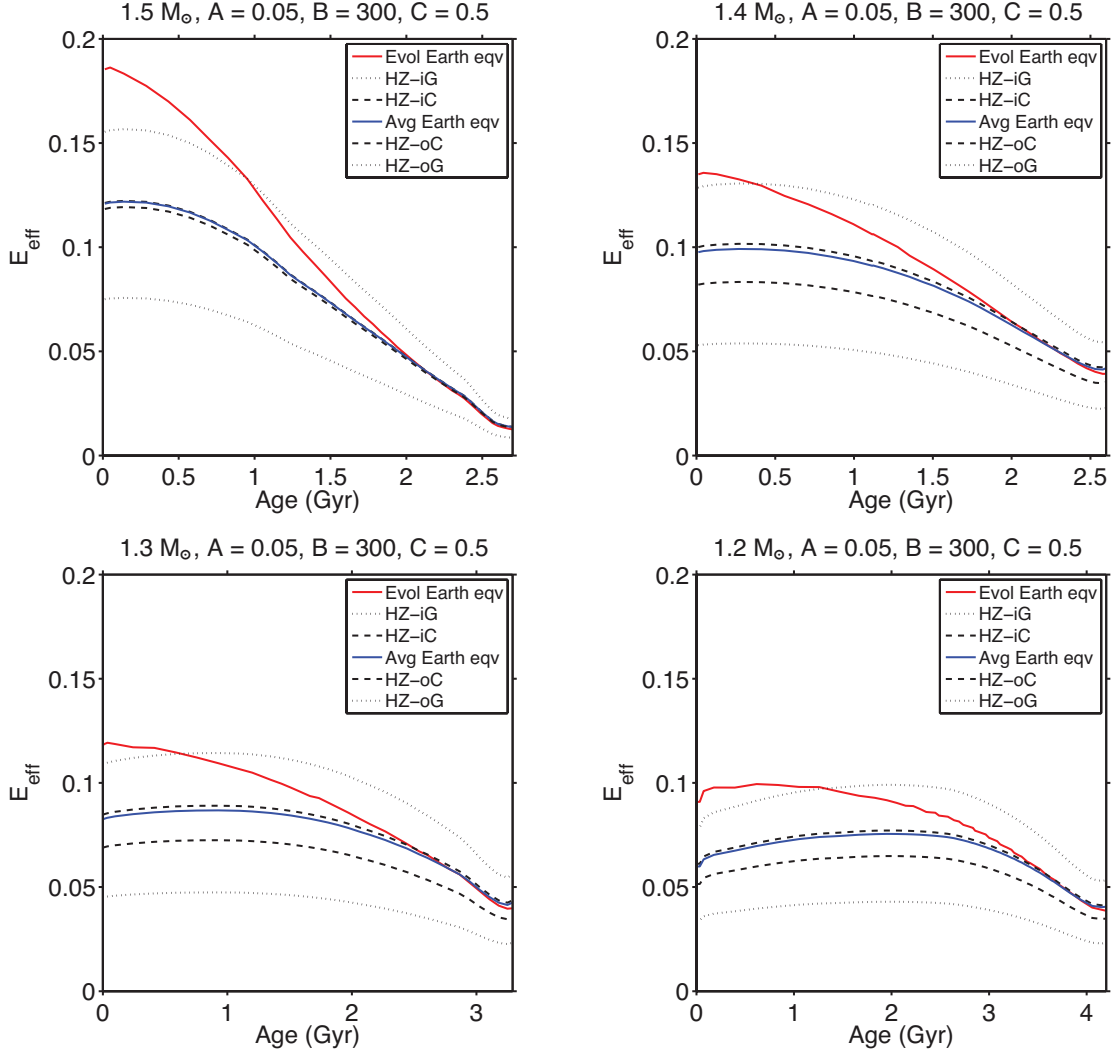


Fig. 12.— Damage inflicted upon DNA at specified positions within the habitable zone of various F-type stars, characterized by their masses, at different ages. Planetary atmospheric attenuation is taken into account with parameters as specified. See Fig. 11 for additional information.

Table 1. F-star reference parameters

Spectral Type	T_{eff} (K)	R_* (R_{\odot})	L_* (L_{\odot})	M_* (M_{\odot})
F0	7200	1.62	6.33	1.60
F2	6890	1.48	4.43	1.50
F5	6440	1.40	3.03	1.25
F8	6200	1.20	1.91	1.10
G0	6050	1.12	1.51	1.05

Table 2. F-star parameters during stellar main-sequence evolution

Age (Gyr)	T_{eff} (K)	L_* (L_{\odot})	Spectral Type ...	T_{eff} (K)	L_* (L_{\odot})	Spectral Type ...	T_{eff} (K)	L_* (L_{\odot})	Spectral Type ...	T_{eff} (K)	L_* (L_{\odot})	Spectral Type ...
$M = 1.2 M_{\odot}$			$M = 1.3 M_{\odot}$			$M = 1.4 M_{\odot}$			$M = 1.5 M_{\odot}$			
0.5	6178	1.770	F8 -22 K	6444	2.644	F5	6720	3.780	F3 +20 K	7084	5.228	F1 +84 K
1.0	6195	1.878	F8	6447	2.839	F5	6682	4.077	F3 -18 K	6983	5.728	F1 -17 K
1.5	6205	1.996	F8	6432	3.036	F5	6589	4.361	F4 +59 K	6775	6.247	F3 +75 K
2.0	6211	2.121	F8 +11 K	6386	3.224	F6 +26 K	6428	4.591	F5 -12 K	6482	6.753	F5 +42 K
2.5	6204	2.247	F8	6303	3.383	F7 +23 K	6218	4.755	F8 +18 K	6117	7.047	F9
3.0	6178	2.366	F8 -22 K	6174	3.493	F8 -26 K
3.5	6130	2.468	F9
4.0	6058	2.555	G0

Note. — For example, an expression such as F8 -22 K means that the stellar effective temperature is 22 K less than that for a standard F8 main-sequence star; for parameters see Hauschildt *et al.* (1999) and subsequent work. Deviations from stellar spectral types are omitted if the difference is found to be less than 10 K.

Table 3. Stellar habitable zones including stellar main-sequence evolution — extreme positions

M_* (M_\odot)	t_{ms} (Gyr)	iG (AU)	iC (AU)	oC (AU)	oG (AU)
1.2	4.255	1.066	1.208	2.174	2.668
1.3	3.291	1.283	1.455	2.511	3.085
1.4	2.605	1.510	1.716	2.888	3.555
1.5	2.706	1.735	1.975	3.581	4.388

Table 4. Stellar habitable zones including stellar main-sequence evolution — continuous domains

M_* (M_\odot)	t_{ms} (Gyr)	iG (AU)	iC (AU)	oC (AU)	oG (AU)
1.2	4.255	1.366	1.548	1.688	2.075
1.3	3.291	1.585	1.796	1.991	2.461
1.4	2.605	1.834	2.079	2.296	2.857
1.5	2.706	2.239	2.535	2.566	3.222